Available online at www.sciencedirect.com
SCIENCE DIRECT
Polymer 47 (2006) 4996–5002
polymer
www.elsevier.com/locate/polymer

The development and characterisation of polyaniline—single walled carbon nanotube composite fibres using 2-acrylamido-2 methyl-1-propane sulfonic acid (AMPSA) through one step wet spinning process

Vahid Mottaghitalab, Geoffrey M. Spinks, Gordon G. Wallace *

ARC Centre of Excellence for Electromaterials Science, Intelligent Polymer Research Institute, University of Wollongong, Northfields Avenue, Wollongong, NSW 2522, Australia

Received 7 January 2006; received in revised form 9 May 2006; accepted 11 May 2006
Available online 6 June 2006

Abstract

High strength, flexible and conductive polyaniline (PANi)–carbon nanotube (SWNT) composite fibres have been produced using wet spinning. The use of dichloroacetic acid (DCAA) containing 2-acrylamido-2-methyl-1-propane sulfonic acid (AMPSA) has been shown to act as an excellent dispersing medium for carbon nanotubes and for dissolution of polyaniline. The viscosity of DCAA–AMPSA solution undergoes a transition from Newtonian to non-Newtonian viscoelastic behaviour upon addition of carbon nanotubes. The ultimate tensile strength and elastic modulus of PANi–AMPSA fibres were increased by 50 and 120%, respectively, upon addition of 0.76% (w/w) carbon nanotubes. The elongation at break decreased from 11 to 4% upon addition of carbon nanotubes, however, reasonable flexibility was retained. An electronic conductivity percolation threshold of ~0.3% (w/w) carbon nanotubes was determined with fibres possessing electronic conductivity up to ~750 S cm^{-1}. Raman spectroscopic evidence confirmed the presence of carbon nanotubes in the polyaniline and also the interaction of the quinoid ring with the nanotubes to provide a doping effect.

Keywords: Polyaniline; AMPSA; Carbon nanotube

1. Introduction

Polymer fibres are readily produced from the insulating emeraldine base (EB) (Scheme 1(a)) or leucoemeraldine base (LEB) forms of polyaniline. They are then rendered conductive by doping using an aqueous acid comprised of small anions [1–6]. The main disadvantage of this approach involves the adverse influence of the acid doping process on mechanical properties. Non-homogenous doping and the possibility of dedoping through diffusion of small anions from the skin of the fibres cause heterogeneities in the fibre structure. Doping of polyaniline in solution, however, results in more homogenous doping and a more uniform material after casting [7].

Doping of polyaniline with sulfonic acids results in an extended coil conformation and a high level of crystallinity resulting in high electronic conductivity [8]. In this regard, a number of studies involving the processing of polyaniline solution blended with sulfonic acids in a suitable solvent have been conducted [9,10]. The production of an electronically conductive emeraldine salt (ES) (Scheme 1(b)) form of polyaniline fibre using 2-acrylamido-2-methyl-1-propane sulfonic acid (AMPSA) (Scheme 1(c)) (in dichloracetic acid) as the dopant has recently been reported [11]. The ultimate tensile strength, elastic modulus and electrical conductivity reported were 97 MPa, 2 GPa and 600 S cm^{-1}, respectively, after annealing of fibres that had been drawn to 5× their original length.

The synthesis and characterisation of PANi–SWNT composites has also been investigated previously [12–15]. Direct dissolution of pristine nanotubes (without chemical functionalization) in aniline can occur via formation of a donor/acceptor charge complex [16]. Using this approach SWNT/PANi composite films have been produced by chemical [17] or electrochemical [18] polymerisation of aniline containing dispersed SWNTs. Alternatively, the SWNTs have been blended with preformed polyaniline in solvents such as *N*-methylpyrrolidone (NMP) [13]. The enhanced electroactivity and conductivity of SWNT/PANi composite

* Corresponding author. Tel.: +61 2 42213127; fax: +61 2 42213114.
E-mail address: gwallace@uow.edu.au (G.G. Wallace).

0032-3861/$ - see front matter © 2006 Elsevier Ltd. All rights reserved.
doi:10.1016/j.polymer.2006.05.037

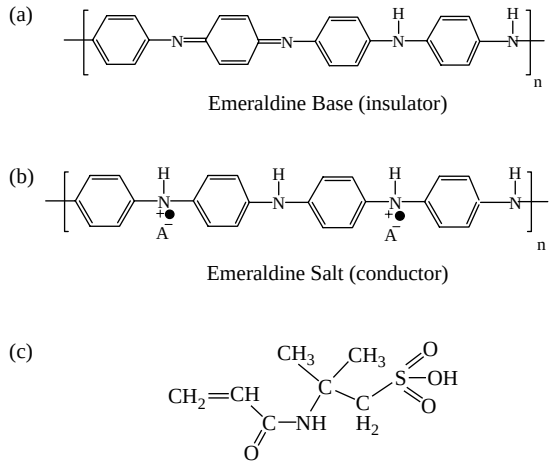

Scheme 1. Structures of (a) PANi (EB), (b) PANi(ES) and (c) AMPSA.

films has been attributed to the strong molecular level interactions that occur between SWNTs and PANi.

In this work, the possibility of producing AMPSA-doped polyaniline fibres containing carbon nanotubes has been investigated. It has been shown that DCAA containing AMPSA and polyaniline provides excellent dispersing power for the SWNTs. The fibres produced from this spinning solution show excellent electronic and mechanical properties suitable for many applications, including artificial muscle fibres.

2. Experimental

2.1. Materials

Polyaniline (PANi, SFST, 280,000 g/mol), dichloroacetic acid (DCAA, Merck, 98%) and 2-acrylamido-2-methyl-1-propane sulfonic acid (AMPSA, Aldrich, 99%) were all used without any further purification. Purified single wall carbon nanotubes (SWNTs, Hipco@CNI) were used as purchased and contained 5 wt% iron residue as determined by elemental analysis.

2.2. Preparation of spinning solution

0.4 g of AMPSA was sonicated for a few seconds in 20 g DCAA to produce a colourless solution. SWNTs (6, 9, 12 or 18 mg) were then added to this solution and sonicated for 30 min. 0.9 g of AMPSA was added to 1.0 g of PANi (EB) powder and this mixture was ground using a mortar and pestle to obtain a grey powder. The resultant powder was added to the previously prepared solution containing SWNTs and AMPSA in DCAA. The solution was continuously stirred over a period of 30 min under a N_2 atmosphere. The spinning solution was stirred for another 30 min at 2000 rpm and 5 °C. Bubbles in the viscous solution were removed using a dynamic vacuum over a period of 1 h. The viscous bubble free solution was transferred to a N_2 pressure vessel to drive the spinning solution through a filter (200 μm, Millipore) then through a single hole spinneret with $L/D=4$ and $D=250$ μm and finally to an acetone coagulation bath at room temperature. In the coagulation bath, the solution solidified and the emerging fibre was taken up on a first bobbin ($D=2.5$ cm) using a linear velocity of 3 m/min. Semi-solid fibres were passed through warm air immediately above a hot plate at 100 °C before being collected by a second bobbin ($D=5$ cm) using a linear velocity of 6 m/min. The fibres were then left at room temperature for at least 30 min prior to the hot drawing process. This involved stretching the as-spun fibre 5× across a soldering iron wrapped with Teflon tape and heated to 100 °C. The fibres were then dried at room temperature for 48 h before characterisation.

2.3. Instrumentation

Fibre samples were cut after cooling in liquid N_2 to obtain circular undamaged cross-sections. Small pieces of fibre were fixed vertically on an aluminium stub using conductive glue. A sputter coater (Dynavac) was used for coating of a thin layer of gold on the cross-section and side wall of the fibres (35 mA for 12 s under 200 mbar Ar). A fully digital LEO Cambridge/Leica Stereoscan 440 Scanning electron microscope (SEM) with tungsten filament using 20 kV beam energy was used for morphological studies of the composite fibres.

The hydrodynamic diameter of carbon nanotubes (SWNTs) solutions were measured using dynamic light scattering (ZS, Malvern, UK). A red laser beam of 632 nm (He/Ne) was used. This system uses the NIBS (non-invasive back scatter) technology where the back scatter at 173 ° is detected. The use of NIBS technology reduces multiple scattering effects since scattered light does not have to travel through the entire sample, so that the size distribution at higher concentrations of sample can be measured.

Dynamic mechanical analysis (DMA) was carried out using a Model Q-800 (thermal analysis). The strain rate mode can be used to collect stress vs. strain data equivalent to that obtained from a universal testing machine. In this mode, a 10 mm gauge length of fibre sample was stretched at a strain rate of 500 μm/min until the sample broke or yielded at 25 °C.

The viscosity of SWNTs solutions was recorded using a Brookfield viscometer (LV-DV II+) using DIN spindle 85 and 87.

In order to measure the conductivity of fibres a homemade four point probe conductivity cell at constant humidity and temperature was employed. The electrodes were circular pins with constant separation of 0.33 cm and fibres were connected to the pins using silver paint (SPI). A constant current was applied between two outer electrodes using a Potentiostat/Galvanostat (Princeton Applied Research Model 363). The potential difference between the inner electrodes was recorded using a digital multimeter 34401A (Agilent).

A three electrode electrochemical cylindrical cell (15 mm× 50 mm) coupled to a Bioanalytical Systems (Model CV27) potentiostat was used for cyclic voltammetry. A 10 mm fibre was used as the working electrode with an Ag/AgCl reference electrode and a Pt mesh counter electrode.

Raman spectra were obtained with the Jobin Yvon Horiba Raman spectrometer model HR800. The spectra were collected with a spectral resolution of 1.8 cm^{-1} in the backscattering mode, using the 632.8 nm line of a He/Ne laser. The nominal power of the laser, polarised 500:1, was 20 mW. A Gaussian/Lorentzian-fitting function was used to obtain band position and intensity. The incident laser beam was focused onto the specimen surface through a 100× objective lens, forming a laser spot ~5 μm in diameter, using a capture time of 50 s. Raman signals were obtained with the half wave plate rotated at 170 ° with a confocal hole set at 1100 μm and the slit set at 300 μm.

3. Results and discussion

For effective integration of carbon nanotubes into a conducting polymer host it is first necessary to achieve a homogenous dispersion in the polymer matrix at weight fractions sufficient enough to allow the percolation threshold to be exceeded. In this regard, a solvent system capable of stabilising the carbon nanotubes and dissolving the polymer matrix is required. The combination of DCAA and AMPSA here resulted in an efficient solvent system for dissolution of polyaniline in the ES form.

The ability of DCAA to act as a dispersant for SWNTs and the effect of the addition of AMPSA on this ability was investigated using the dynamic light scattering technique. The hydrodynamic diameter distribution for DCAA–SWNT (0.05% (w/w)) solutions containing 0–2% (w/w) AMPSA was determined (Fig. 1).

DCAA–SWNT samples containing AMPSA showed lower hydrodynamic diameters compared to neat DCAA–SWNT, indicating that AMPSA assists in de-bundling of SWNTs. The addition of AMPSA also assists in stabilising SWNT dispersions in DCAA. The resulting dispersions were stable for more than 1 day; neither sedimentation nor aggregation of nanotube bundles was observed in the samples. Conversely, in samples that did not contain AMPSA aggregation of particles was observed after 1 h, as confirmed by the dynamic light scattering technique. The increased stability of the SWNT dispersions after addition of AMPSA was presumably due to interaction of SWNTs and AMPSA, resulting in increased electrostatic repulsion and reduced aggregation [19–21].

Ultrasonication is necessary for dispersion of SWNTs, however, Zakri [22] has shown that increased sonication time significantly reduces the length of carbon nanotubes and the conductivity of fibres produced from them. It has also been shown that the aspect ratio of nanotubes has a significant impact on the tensile strength of composites containing them [23], reinforcing the importance of maintaining tube length by minimising sonication time. The influence of sonication time on the homogeneity of SWNT dispersions was monitored using viscometry. At shorter sonication times significant random fluctuations in viscosity are observed with shear rate, indicating that the dispersion was not fully homogenised. It was found that at least 30 min of sonication was required to remove these

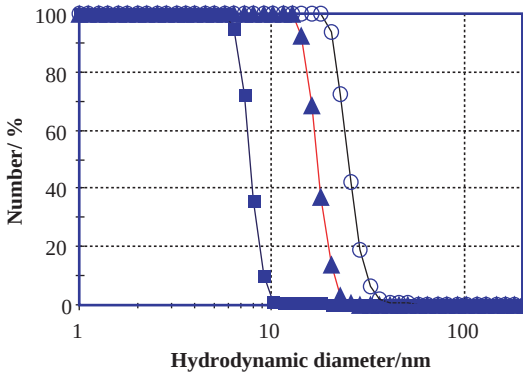

Fig. 1. Influence of concentration of AMPSA in DCAA on hydrodynamic diameter of SWNTs (0.05% (w/w)). AMPSA concentration was varied between (○) 0%, (▲) 1% and (■) 2% (w/w). Hydrodynamic diameters were determined 30 min after sonication.

fluctuations and to obtain a homogeneous dispersion of SWNTs.

An understanding of the rheological properties of dispersions can be used to determine the optimum composition for wet spinning and as a useful tool for prediction of interconnectivity of nanotube bundles in the matrix after addition of polymer [24–26]. Fig. 2 shows the viscosity vs. shear rate plots obtained as a function of increasing SWNT content. For successful wet spinning, a viscosity of 2000–3000 cP is required [27]. A number of parameters needed to be optimised to achieve this viscosity while also achieving the desired loadings of SWNTs and AMPSA. Using a feed solution containing a mole ratio of 1:0.6 for PANi:AMPSA has been shown to result in polyaniline fibres with high conductivity, [11,28] so this ratio was maintained in the present study.

It was also found that a concentration of approximately 10% (w/w) PANi-ES in DCAA was required to achieve the desired solution viscosity. Addition of carbon nanotubes to the spinning solution significantly increased viscosity at low shear rates (Fig. 2).

However, the viscosity of these dispersions decreased rapidly with increasing shear rates. At the shear rate estimated for fibre spinning (10^2–10^3 s^{-1}), the viscosities of all SWNT–

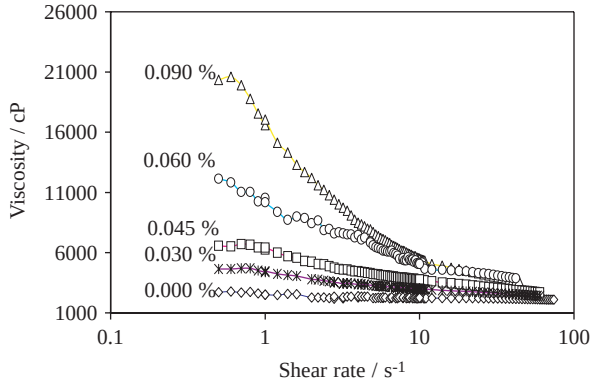

Fig. 2. The influence of carbon nanotube content on the viscosity of solutions containing PANi–AMPSA (11.5% (w/w)). The weight fraction of SWNT is given with respect to the weight of DCAA solvent.

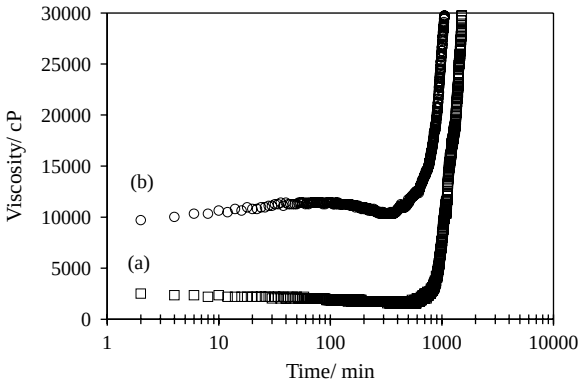

Fig. 3. Viscosity vs. time up to gelation for solutions containing (a) PANi/AMPSA in DCAA (11.5% (w/w)), (b) as in (a) but with 0.09 % (w/w) SWNTs added.

PANi–DCAA dispersions were very similar and in the range required. The higher viscosity and shear thinning behaviour observed for SWNT dispersions suggested that the SWNTs aided in forming entanglements with the polymer chains. Specific interactions between the SWNTs and the PANi are considered below.

Another relevant issue for fibre spinning of PANi is gelation of the feed solution, which renders it unsuitable for fibre spinning. The viscosity of the feed solution vs. time was determined (Fig. 3). It was found that solutions containing either neat PANi–AMPSA or with 0.09% (w/w) SWNTs added gelled after 10 or 6.5 h, respectively. Gelation times for all other SWNT contents were between 7 and 10 h. All dispersions were sufficiently stable to allow enough time for spinning prior to gelation.

The use of feed solutions containing 0.03–0.09% (w/w) SWNTs in DCAA resulted in formation of continuous fibres with reasonable mechanical properties (Table 1). SWNT loadings are given as weight fractions with respect to the weight of PANi–AMPSA in solid fibres. For fibres containing 0.76% (w/w) SWNT, a 50% increase in tensile stress (σ_b), a 120% increase in Young's modulus (E) and a 40% decrease in elongation at break (ε_b) compared with neat PANi fibres were observed. The improvement in mechanical properties of fibres with the addition of SWNTs is illustrated by the stress–strain curves given in Fig. 4.

Ramamurthy and his colleagues [29] investigated the influence of addition of MWNTs to PANi films fabricated by solution processing. Physical characterization of these composites by tensile testing and dynamic thermal mechanical analysis indicated that PANi containing 1% w/w MWNTs is more mechanically and thermally stable than polyaniline itself.

Table 1
Influence of SWNTs loading on mechanical properties of PANi–AMPSA fibres

% (w/w) SWNT in PANi–AMPSA	σ_b (MPa)	E (GPa)	ε_b (%)
0.00	170±22	3.4±0.4	9±3
0.26	196±17	3.9±0.4	8±3
0.38	199±9	5.6±0.3	7±2
0.52	229±28	6.2±0.3	7±2
0.76	255±32	7.3±0.4	4±1

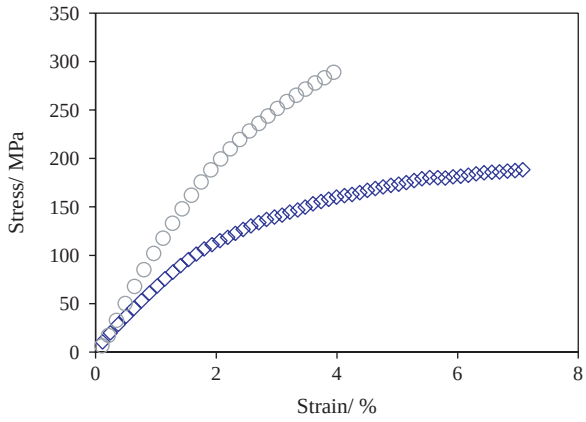

Fig. 4. Typical stress–strain curves for (♦) neat PANi–AMPSA and (○) PANi–AMPSA–SWNT (0.76 % (w/w) SWNTs).

However, only marginal improvements in mechanical properties were reported.

SEMs of the cross-sections of fibres containing no SWNTs and 0.76% (w/w) SWNTs are illustrated in Figs. 5 and 6, respectively. In both cases, uniform and non-porous fibres were produced.

Although the strain at break decreases considerably with increasing carbon nanotube content, knots formed in PANi–AMPSA fibers with or without SWNTs showed high degrees of flexibility, as demonstrated in the SEMs in Fig. 7(a) and (b). The fiber containing nanotubes also shows high level of twistability (i.e. 36 twist per inch (TPI)) in S (counter clock wise) and Z (clockwise) styles, which is essential to enable the fiber to form a strong thread to be as warp or woof in textile matrix (Fig. 7(c) and (d)).

Since the processing parameters including take-up, drawing and thermal stretching ratio were the same for all fibres, the improvement of mechanical properties with the addition of SWNTs could be attributed mainly to reinforcing of the PANi matrix through load transfer to oriented nanotube ropes. It has been shown that the formation of a crystalline coating around carbon nanotube bundles can assist load transfer by improving the adhesion between the polymer and nanotubes [23]. However, X-ray diffraction studies showed no evidence of crystallinity in the composite fibers produced here [30,31].

The effect of SWNT addition to PANi fibres on conductivity was also investigated (Fig. 8). A percolation threshold of ~0.35% (w/w) SWNTs was determined using the basic percolation power law [32]. The value for conductivity

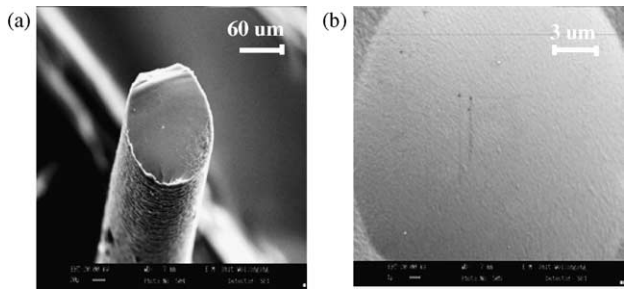

Fig. 5. Cross-sectional SEM of neat PANi–AMPSA fibre. Scale bar (a) 20 μm (b) 1 μm.

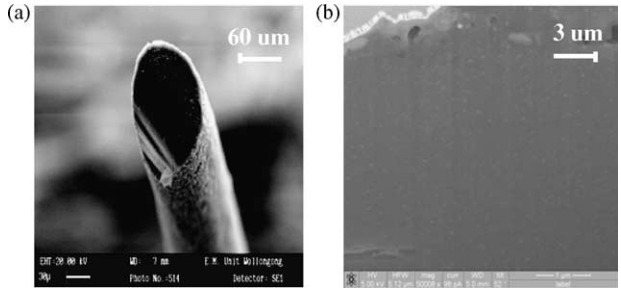

Fig. 6. Cross-sectional SEM of PANi–AMPSA–SWNT (0.76% (w/w) SWNTs) fibre. Scale bar (a) 30 μm (b) 1 μm. Inner core was sectioned by ion beam grinder.

percolation threshold obtained here is in good agreement with another polymer-nanocomposite system that showed a 0.5 w/w % percolation level [33]. In addition, a significant increase in electrical conductivity was observed even at low SWNTs loadings, while the neat PANi–AMPSA fibres prepared here had similar conductivities ($\sim$500 S cm^{-1}) compared to those obtained in a previous study (600 S cm^{-1}) [11].

A number of workers have investigated the addition of carbon nanotubes to PANi on the subsequent electrical properties [12,14,34–37]. For example, Yu and co-workers [34] reported that the addition of MWNTs (1% w/w) to polyaniline increased the conductivity by an order of magnitude. Using a similar approach Deng and co-workers [14] prepared PANi with SWNT loadings using in situ emulsion polymerization. The conductivity of the resultant composite containing 10% w/w SWNT was 6.6×10^{-2} S cm^{-1}, which was more than 25 times that obtained for the neat PANi (2.6×10^{-3} S cm^{-1}) using the same synthesis conditions. PANi produced in the presence of functionalized (carboxy containing groups) MWNTs also showed a 50–70% higher conductivity than PANi without the nanotubes [36]. Addition of SWNTs to PANi after polymer synthesis has also been shown to significantly enhance conductivity [35,12].

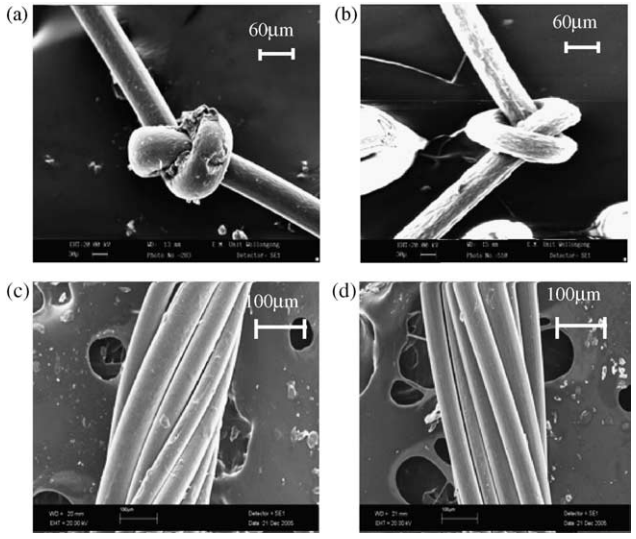

Fig. 7. SEMs of knotted (a) PANi–AMPSA and (b) PANi–AMPSA–SWNT (0.76% (w/w) SWNTs). 16 ply twisted fiber (TPI = 36) of PANi–AMPSA–SWNT (0.76% w/w) with (c) S shaped twisting(d) Z shaped twisting.

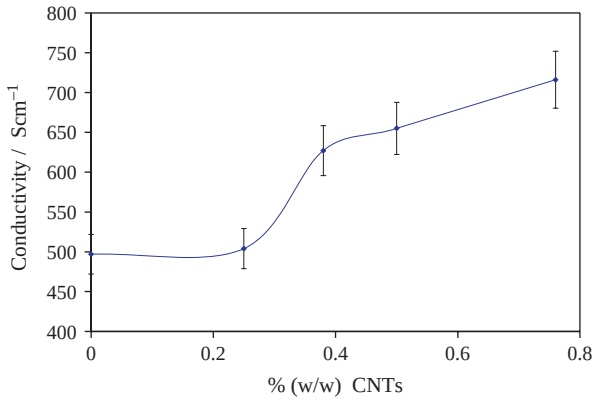

Fig. 8. Electrical conductivity of PANi–AMPSA–SWNT composite fibres as a function of carbon nanotube loading.

Raman spectroscopy was used to provide evidence of the interaction between carbon nanotubes and the PANi in the composite fibres prepared here (Fig. 9). The important features of the Raman spectra for singe walled carbon nanotubes (SWNTs) (Fig. 9(f)) occur in the range 200–2700 cm^{-1}. The radial breathing mode (RBM) is observed in the range 170–300 cm^{-1} and gives information on nanotube diameter and chirality.

The tangential G band observed at 1594 cm^{-1} originates from the graphite like structure, while the disorder (D) band and its second order harmonic known as the D* band appear at 1309 and 2604 cm^{-1}, respectively. As shown in Fig. 9, Raman absorption peaks due to SWNTs increased in intensity when

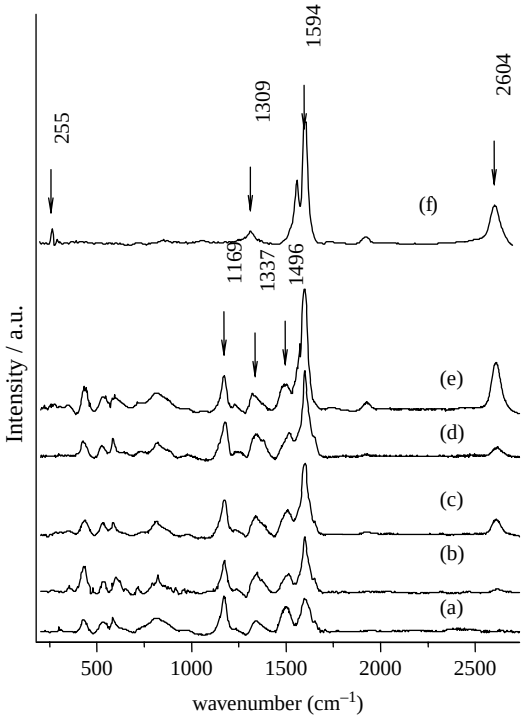

Fig. 9. Enhanced Raman spectra (λ_{exc} = 632.8 nm) obtained for PANi–AMPSA–SWNT composite fibres containing various SWNT loadings (a) 0% (w/w), (b) 0.26% (w/w), (c) 0.38% (w/w), (d) 0.52% (w/w), (e) 0.76% (w/w) and (f), Enhanced Raman spectrum of SWNTs bucky paper.

Table 2
Assigned Raman absorption frequencies originating from PANi–AMPSA–SWNT composite fibres

Raman shift	Assignment
2604	D* band of SWNTs
1594	G band of SWNT-C–C stretching of benzoid ring
1496	C–N stretching of benzoid ring
1337	C–$N^{\cdot +}$ stretching of bipolaron structure
1169	C–H stretching of benzoid ring
190–255	(RBM) SWNTs

λ_{exc} = 632.8 nm.

more nanotubes were incorporated into the fibres. Similar observations have been made previously [13]. A summary of assigned Raman absorption frequencies for PANi–SWNTs composite fibres is provided in Table 2.

Raman spectra can reveal information regarding the interaction between SWNTs and polyaniline. The dissolution of EB PANi in DCAA–AMPSA resulted in the formation of the ES form of PANi, as described previously [38,39] (bands at 1337, 1496, 1592 cm^{-1}). The peak at 1337 cm^{-1} corresponding to the bipolaron (C–$N^{\cdot +}$) band of ES PANi was further enhanced by addition of carbon nanotubes, suggesting an increase in doping level [37,40]. With increased SWNT loading a decrease in the ratio of absorption of the intensity of the 1496 cm^{-1} band (C–N stretching of benzoid ring) compared to the 1169 cm^{-1} band (C–H stretching of benzoid ring) was observed. This could be attributed to site selective interaction of PANi and SWNTs [37]. Such behaviour in polyaniline fibers has been observed previously in studies involving the introduction of SWNTs after spinning [31]. According to previous studies by Do Nascimento and co-workers [41] the presence of the D band at 2604 cm^{-1} suggests that some metallic SWNTs do not interact strongly with the PANi backbone.

Cyclic voltametry for the neat PANi fibre and PANi–SWNT (0.76% (w/w) SWNTs) composite fibre in 1 M HCl is shown in Fig. 10. To avoid the pernigraniline oxidation state and subsequent degradation, the potential range was limited to between −0.2 and 0.5 V. This potential range covers the first redox process of polyaniline, that is the transition from the leucoemeraldine to the emeraldine oxidation state. For the fibre containing SWNTs, the oxidation/reduction responses (attributed to the polyaniline redox chemistry) are better defined when compared with the neat PANi fibre. The oxidation potential (+0.3 V) shifted to a lower value (+0.2 V) with addition of nanotubes. However, the reduction peak was only slightly changed with the addition of carbon nanotubes. The presence of the carbon nanotubes obviously facilitates the transition from the less conductive leucoemeraldine state to the emeraldine state.

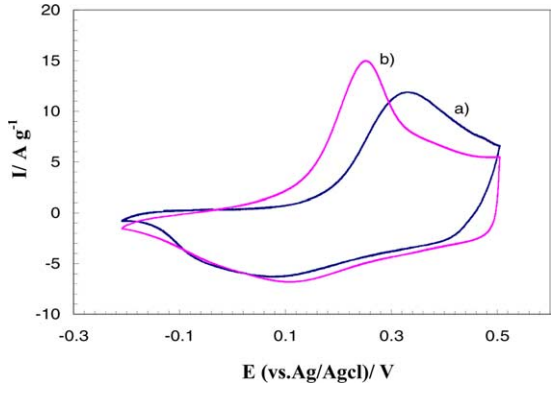

Fig. 10. Cyclic voltammograms of (a) neat PANi–AMPSA and (b) SWNT-reinforced PANi–AMPSA fibres. Potential was scanned between −0.2 V and +0.5 V (vs. Ag/AgCl) in 1 M $HCl_{(aq)}$ at 5 m Vs^{-1}.

4. Conclusions

The addition of carbon nanotubes to PANi–AMPSA fibres processed from dichloroacetic acid resulted in materials with high conductivity, high mechanical strength and modulus. Conductivities as high as 750 S cm^{-1} were achieved in continuously spun fibres up to 50–100 m in length. Tensile strength of 250–300 MPa and moduli of 7–8 GPa for PANi–SWNT composite fibres were approximately two times higher than for neat PANi fibre. The fibres produced were tough enough to be knotted or twisted. Electroactivity was enhanced by the addition of nanotubes, as shown by cyclic voltammetry.

AMPSA in dichloroacetic acid was shown to be a highly effective dispersant for carbon nanotubes. Rheological studies and Raman spectroscopy studies indicated strong interactions between the SWNTs and the PANi. These interactions very likely contributed to the effective transfer of load and charge between the PANi matrix and the SWNT fibres.

The unique properties of high strength, robustness, good conductivity and pronounced electroactivity make these fibres potentially useful in many electronic textile applications. PANi–SWNTs composite fibres are currently being considered for application in artificial muscles, sensors, batteries and capacitors.

Acknowledgements

The financial support of the Australian Research Council is gratefully acknowledged.

References

[1] Mattes BR, Wang HL, Yang D, Zhou YT, Blumenthala WR, Hundeleya MF. Synth Met 1997;84(1–3):45–9.
[2] Chacko AP, Hardaker SS, Gregory RV. Polym Prepr 1997;38(2):367–8.
[3] Chacko AP, Hardaker SS, Gregory RV. Polym Prepr 1996;37(2):743–4.
[4] Mattes BR, Wang H-L, Yang D. ANTEC Conf Proc 1997;2:1463–7.
[5] Gregory RV. ANTEC Conf Proc 1995;2:1683–7.
[6] Scherr EM, MacDiarmid AG, Manohar SK, Masters JG, Sun Y, Tang X, et al. Synth Met 1991;41–43(1–2):735–8.
[7] Cao Y, Smith P, Heeger AJ. Synth Met 1992;48(1):91–7.
[8] Holland ER, Pomfret S, Adams PN, Monkman AP. J Phys: Condens Mater 1996;8:2991–3003.
[9] Pomfret SJ, Adams PN, Comfort NP, Monkman AP. Adv Mater 1998; 10(16):1351–3.
[10] Wang YZ, Joo J, Hsu CH, Epstein AJ. Synth Met 1995;69(1–3):267–8.

[11] Pomfret SJ, Adams PN, Comfort NP, Monkman AP. Polymer 2000;41(6):2265–9.
[12] Zengin H, Zhou W, Jin J, Czerw R, Smith Jr DW, Echegoyen L, et al. Adv Mater 2002;14(20):1480–3.
[13] Baibarac M, Baltog I, Lefrant S, Mevellec JY, Chauvet O. Chem Mater 2003;15(21):4149–56.
[14] Deng J, Ding X, Zhang W, Peng Y, Wang J, Long X, et al. Eur Polym J 2002;38(12):2497–501.
[15] Huang JE, Li XH, Xu JC, Li HL. Carbon 2003;41(14):2731–6.
[16] Sun Y, Wilson SR, Schuster D. J Am Chem Soc 2001;123(22):5348–9.
[17] Li XH, Wu B, Huang JE, Zhang J, Liu ZF, Li HI. Carbon 2002;41(8):1670–3.
[18] Huang JE, Li XH, Xu JC, Li HL. Carbon 2003;41(14):2731–6.
[19] Matarredona O, Rhoads H, Li Z, Harwell JH, Balzano L, Resasco DE. J Phys Chem B 2003;107(48):13357–67.
[20] Sabba Y, Thomas EL. Macromolecules 2004;37(13):4815–20.
[21] Islam MF, Rojas E, Bergey DM, Johnson AT, Yodh AG. Nano Lett 2003;3(2):269–73.
[22] Badaire S, Poulin P, Maugey M, Zakri C. Langmuir 2004;20(24):10367–70.
[23] Coleman JN, Cadek M, Blake R, Nicolosi V, Ryan KP, Belton C, et al. Adv Funct Mater 2004;14(8):791–8.
[24] Potschke P, Fornes TD, Paul DR. Polymer 2002;43(11):3247–55.
[25] Wagener R, Reisinger TJG. Polymer 2003;44(24):7513–8.
[26] Du F, Scogna RC, Zhou W, Brand S, Fischer JE, Winey KI. Macromolecules 2004;37(24):9048–55.
[27] Qi B, Mattes BR. Resistive heating using polyaniline fibre, US patent, 60/430,728, USA, 2002.
[28] Lu W, Mattes BR. J Electrochem Soc 2003;150(9):E416–E22.
[29] Ramamurthy PC, Harrell WR, Gregory RV, Sadanadan B, Rao AM. J Electrochem Soc 2004;151:G502–G6.
[30] Yu Y, Che B, Si Z, Li L, Chen W, Xue G. Synth Met 2005;150:271–7.
[31] V. Mottaghitalab 'Development and characterization of polyaniline–SWNT conducting composite fibers', University of Wollongong, Wollongong, PhD thesis, 2006.
[32] Kirkpatrick S. Rev Mod Phys 1973;45(12):574–9.
[33] Du F, Scogna RC, Zhou W, Brand S, Fischer JE, Winey KI. Macromolecules 2004;37(24):9048–55.
[34] Yu Y, Che B, Si Z, Li L, Chen W, Xue G. Synth Met 2005;150:271–7.
[35] Ramamurthy PC, Harrell WR, Gregory RV, Sadanadan B, Rao AM. Synth Met 2003;137:1497–8.
[36] Wu T-M, Lin Y-W, Liao C-S. Carbon 2005;43:734–40.
[37] Cochet M, Maser WK, Benito AM, Callejas MA, Martinez MT, Benoit JM, et al. Chem Commun 2001;1450–1.
[38] Pereira da Silva JE, Temperini MLA, Cordoba de Torresi SI. Electrochim Acta 1999;44(12):1887–91.
[39] Pereira da Silva JE, de Faria DLA, Cordoba de Torresi SI, Temperini MLA. Macromolecules 2000;33(8):3077–83.
[40] Mottaghitalab V, Spinks GM, Wallace GG. Synth Met 2005;152(1–3):77–80.
[41] Do Nascimento GM, Corio P, Novickis RW, Temperini MLA, Dresselhaus MS. J Polym Sci, Part A: Polym Chem 2005;43:815–22.